



## R-curve behavior and roughness development of fracture surfaces

STÉPHANE MOREL<sup>1</sup>, ELISABETH BOUCHAUD<sup>2</sup>, JEAN SCHMITTBUHL<sup>3</sup> and  
GÉRARD VALENTIN<sup>1</sup>

<sup>1</sup>Laboratoire de Rhéologie du Bois de Bordeaux, UMR 5103, Domaine de l'Hermitage, B.P.10, 33610 Cestas  
Gazinet, France

<sup>2</sup>C.E.A. Saclay, (D.S.M./D.R.E.C.A.M./S.P.C.S.I.), 91191 Gif-Sur-Yvette Cedex, France

<sup>3</sup>Laboratoire de Géologie, UMR 8538, Ecole Normale Supérieure, 24 rue Lhomond, 75231 Paris Cedex 05,  
France

Received 5 June 2001; accepted in revised form 7 January 2002

**Abstract.** We investigate the idea that the fractal geometry of fracture surfaces in quasibrittle materials such as concrete, rock, wood and various composites can be linked to the toughening mechanisms. Recently, the complete scaling analysis of fracture surfaces in quasibrittle materials has shown the anisotropy of the crack developments in longitudinal and transverse directions. The *anomalous* scaling law needed to describe accurately these particular crack developments emphasizes the insufficiency of the fractal dimension, usually used to characterize the morphology of fracture surfaces. It is shown that a fracture surface initiating from a straight notch, exhibits a first region where the amplitude of roughness increases as a function of the distance to the notch, and a second one where the roughness saturates at a value depending on the specimen size. Such a morphology is shown to be related to an *R*-curve behavior in the zone where the roughness develops. The post *R*-curve regime, associated with the saturation of the roughness, is characterized by a propagation at constant fracture resistance. Moreover, we show that the main consequence of this connection between anomalous roughening at the microscale and fracture characteristics at the macroscale is a material-dependent scaling law relative to the critical energy release rate. These results are confirmed by fracture experiments in Wood (Spruce and Pine).

**Key words:** Fractal cracks, fracture energy release, quasibrittle materials, *R*-curve, scaling, size effect, toughening.

### 1. Introduction

Quasibrittle materials, such as concrete, rock, tough ceramics, wood and various composites, exhibit an extensive microcracking in a limited area – known as the fracture process zone –, located just ahead and around the tip of a main crack. Contrary to the case of ductile fracture of metals in which the fracture process zone is negligible in size compared to the non linear plastic-hardening zone, in a quasibrittle material the process zone is large while the plastic-hardening zone is negligible. At a micromechanical level, the main effect of the microcracking is a decrease of the singular stress field induced by energy dissipative mechanisms and stress redistribution which occurs from the elastic interactions of the main crack with the microcracks and of the microcracks with each other (Hori and Nemat-Nasser, 1987; Kachanov, 1994; Brencich and Carpinteri, 1998). This shielding affects the main crack and results, at a macroscopic level, in an apparent increase of the toughness (*toughening by microcracks*): damage is at the origin of the so-called phenomenological *R*-curves (Lawn, 1993). One important consequence of this particular behavior is the size effect. Moreover, at a microscopic level, profuse microcracking induces additional loading modes on the main crack which are responsible for the local macrocrack deflections (Hori and Nemat-Nasser, 1987; Ducourthial et al., 2000) and

hence, for the roughness of the main fracture surface. Because of the tortuosity of the fracture path, the real fracture surface can subsequently increase the effective fracture energy and may be a potential source of toughening. Thus, when a quantitative analysis of fracture surfaces has been possible because of considerable progresses in fractal characterization of rough growth processes, it was expected to correlate the measured roughness to macroscopic mechanical properties such as fracture energy or toughness.

Since the early work of Mandelbrot et al. (1984), the study of the morphology of fracture surfaces is nowadays a very active field of research. Observations have shown that, within a certain range of lengthscales, the fracture surfaces in many materials, and especially in brittle and quasibrittle materials exhibit self-affine characteristics (Feder, 1988; Bouchaud, 1997). However, these studies concern only several parallel topographic profile generally recorded in the direction perpendicular to crack propagation. The complete morphologies of the fracture surfaces of quasi-brittle materials (granite: López and Schmittbuhl, 1998; wood: Morel et al., 1998) have been reported only recently, through the study of topographic maps composed of tens or hundreds of parallel profiles. It has been shown that the crack development is anisotropic, i.e., different in the crack propagation direction and transverse to it. To describe this anisotropy, one needs to introduce three scaling exponents (for instance the *anomalous* scaling: López and Rodríguez, 1996). This shows the insufficiency of the fractal dimension in this case.

In this paper, mode I fracture tests made on geometrically similar quasibrittle (wood) fracture specimens of various sizes are reported. In Section 2, the *R*-curves are derived from the load-displacement curves, and a pronounced size effect on the critical energy release rates is observed. The roughness analysis (Morel et al., 1998) of the fracture surfaces is summarized in Section 3. An anomalous scaling law is used to accurately describe the morphology of these surfaces and especially the roughness development. At the onset of fracture, the magnitude of the roughness increases as a function of the distance to the notch, whereas, far from the notch, the magnitude remains constant and function of the specimen size. The link between crack morphology and fracture mechanics is finally discussed in Section 4. Many attempts were made in the past to re-write the Griffith criterion taking into account the self-affine nature of the fracture surface, leading to connections between the fracture toughness and either the fractal dimension (Mosolov, 1993; Carpinteri, 1994; Balankin, 1996; Borodich, 1997; Bažant, 1997) or relevant length scales (Bouchaud and Bouchaud, 1994). In this paper, we incorporate into the Griffith criterion the complete description of the fracture surface on the basis of an anomalous scaling. We show that fracture equilibrium leads to a fracture resistance that increases with the crack length, i.e. to an *R*-curve behavior. Moreover, we show that the connection between the fractal geometry of cracks and the material fracture properties leads to a size effect on the critical energy release rate. We show that the predicted *R*-curves and size effects are very consistent with experimental measurements obtained on wood.

## 2. Experiment

In the following the experimental setup of the mode I fracture tests on a quasibrittle material is described. Two wood species have been tested: Maritime pine (*Pinus pinaster Ait*) and Norway spruce (*Picea Abies L.*). The average oven dry specific densities were, respectively, 0.55 and 0.40 and the moisture content of all specimens was measured between 11 and 13%. Tests were made on modified tapered double cantilever beam specimens (TDCB) oriented along

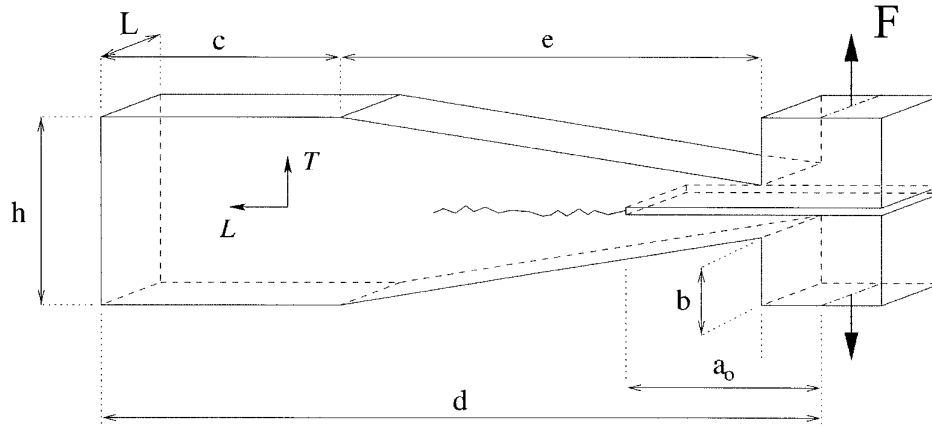


Figure 1. Modified tapered double cantilever beam (TDCB) specimen (see Table 1).

Table 1. Dimensions of TDCB specimens (in mm) (see Figure 1).

$L$	$d$	$a_0$	$h$	$b$	$c$	$e$
7.5	140	40	25	7.5	60	70
11.3	210	60	37.5	11.3	90	105
15	280	80	50	15	120	140
22.5	420	120	75	22.5	180	210
30	560	160	100	30	240	280
60	1120	320	200	60	480	560

the longitudinal-tangential directions of wood. Six sets of geometrically similar specimens characterized by their width ( $L$ ): 7.5, 11.3, 15.0, 22.5, 30.0 and 60.0 mm have been used (Figure 1). A straight notch is machined with a band saw (thickness 2 mm) and prolonged a few millimeters with a razor blade (thickness 0.2 mm). The dimensions of the specimens are given in Table 1. A fracture is propagated from the notch with a uniaxial tension at a constant opening rate.

The tapered shape of the specimens imposes a mode I stable crack growth (Morel, 1998). The fracture surfaces are generated along the average longitudinal-radial plane. During the tests, load-deflection values were continuously recorded.

During fracture tests on a quasibrittle material such as wood, a fracture process zone (where microcracks nucleate, grow and coalesce) starts to grow as the load increases while remaining attached to the tip of the notch. The non linear plastic-hardening zone being negligible in size compared the fracture process zone, the unloading irreversibility is unimportant and hence, a quasibrittle material can be described by a linear elastic fracture mechanics (LEFM) approach in the sense of an equivalent linear elastic problem (Bažant and Kazemi, 1990) where the structure is assumed to be linear elastic everywhere and where the crack lengths can be estimated from the unloading compliance of the specimen. This requires a computation of the elastically equivalent crack lengths which give, according to LEFM, the same experimental unloading compliances. The dependence of the compliances on the equivalent crack length

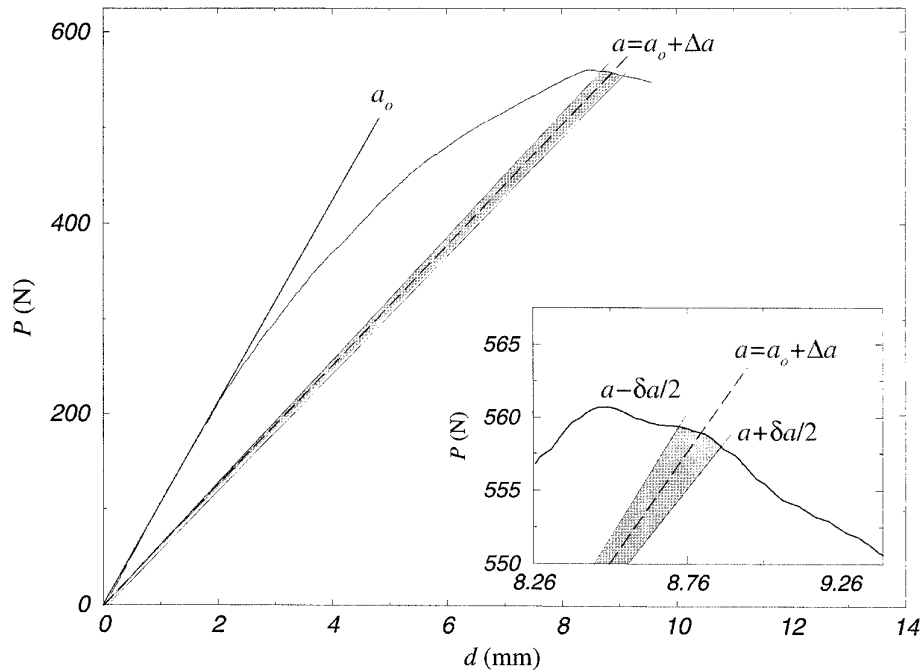


Figure 2. Method for the determination of the elastic energy release rate  $G_R = A/(\delta aL)$  where  $A$  is the elastic energy release corresponding to the filled area. The crack lengths are determined from the compliances and the small crack extension  $\delta a$  has been fixed to  $\delta a = 0.3$  mm.

have been computed using a finite element method (Morel, 1998) for the TDCB specimen geometry and with the elastic characteristics of both wood species. On this basis, the elastic energy release rates  $G_R$  are estimated from the load-deflection curves for any crack length increment  $\Delta a$  (defined as the crack length extension :  $\Delta a = a - a_0$  where  $a$  is the equivalent crack length and  $a_0$  is the length of the initial notch).

For a given crack length increment  $\Delta a$  (Figure 2), the elastic energy release rate  $G_R$  is determined from the elastic energy released during a small crack propagation  $\delta a$  (corresponding to the filled area in Figure 2) related to the corresponding small cracked surface  $\delta aL$  ( $L$  being the width of the specimen). Figures 3a and 3b show the evolution of the energy release rate  $G_R$  as a function of the crack length extension  $\Delta a$  obtained respectively for a small ( $L = 7.5$  mm) and a large ( $L = 60.0$  mm) TDCB specimen of Maritime Pine. For both specimen dimensions, a pronounced *R*-curve behavior is observed, i.e., an evolution of the resistance to crack growth as a function of the equivalent crack length increment (Lawn, 1993). After a characteristic propagation distance (about 9 mm in the case of the small specimen and 65 mm in the case of the large one) which corresponds approximately to the peak load, the resistance to crack growth becomes independent of the crack length increment  $\Delta a$ . Thus, the postpeak crack propagation arises at constant resistance and defines a *critical* value of the resistance denoted  $G_{RC}$  (Figure 3). The same kind of fracture behavior (i.e., *R*-curve and post *R*-curve regime at constant resistance to crack growth) has been observed also on Norway Spruce.

Figures 4a and 4b show respectively, for Maritime Pine and Norway Spruce specimen sets, the size effect on measured  $G_{RC}$  values. Despite the limitation of the range of sizes used ( $7.5 \leq L \leq 60.0$  mm), which is narrower than a decade (a larger range of sizes is very

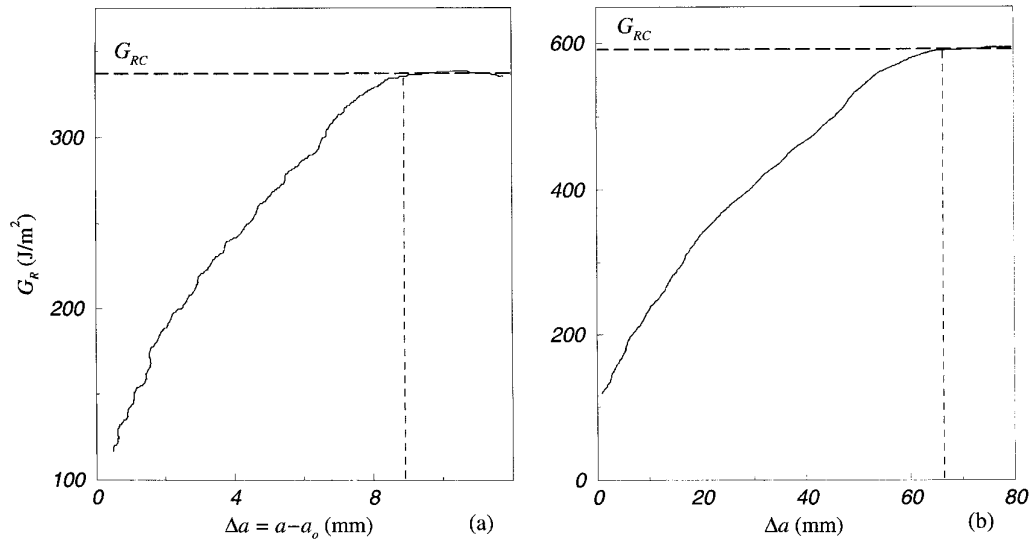


Figure 3. R-curves measured on a small specimen ( $L = 7.5$  mm (a)) and on a large one ( $L = 60.0$  mm (b)) in the case of Maritime Pine. The horizontal **asymptote** corresponds to the critical value of the resistance to crack growth  $G_{RC}$  and is related to the postpeak crack propagation.

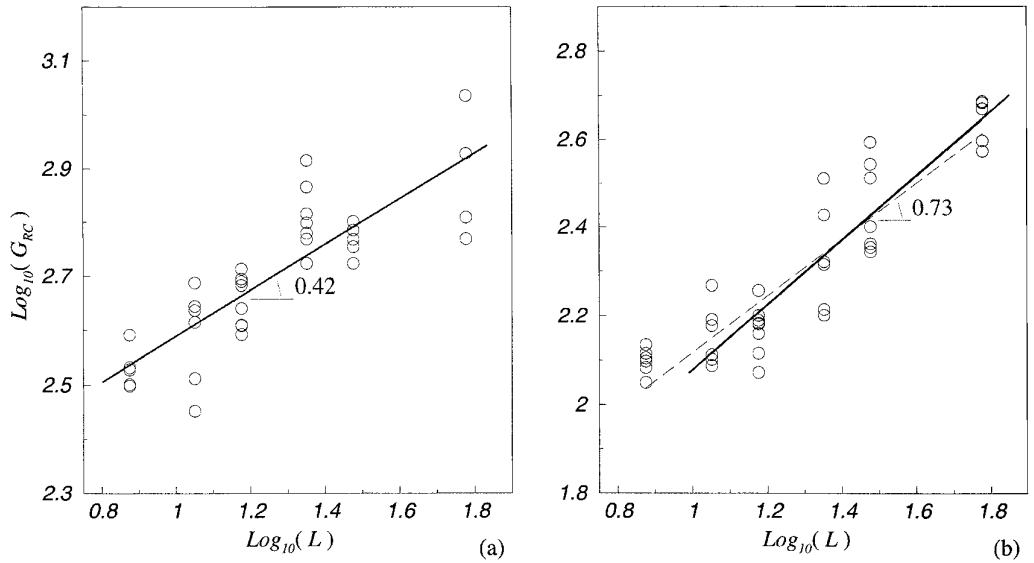


Figure 4. Size effect on the critical energy release rate measured on Maritime Pine (a) and Norway Spruce (b). A power law fit of the data,  $G_{RC} \sim L^\alpha$ , gives an exponent  $\alpha = 0.42$  for Pine specimens and  $\alpha = 0.73$  for Spruce specimens.

difficult to obtain on wood), the experimental critical resistances show a pronounced increase as a function of the specimen sizes. The scattering of these critical resistances is due to the natural variability of the elastic characteristics of wood. This point will be discussed in the following. For both wood species, the evolutions of the critical resistance to crack growth are fitted by a power law  $G_{RC} \sim L^\alpha$ . For Maritime Pine, the size effect on the critical resistance is characterized by an exponent  $\alpha = 0.42$  while for Norway Spruce  $\alpha = 0.73$  is obtained. Note that the smallest Spruce specimens ( $L = 7.5$  mm, Figure 4b) have an oven dry specific density larger than the average density measured on the other specimens. This set of specimens is not representative of an *average Norway Spruce sort*, and hence, is excluded from the fit. Otherwise, the critical energy release rates measured on Pine are larger than the one measured on Spruce but the size effect is stronger in Spruce.

### 3. Anomalous roughening of fracture surfaces

From the early work of Mandelbrot et al. (1984), many efforts have been devoted to the statistical characterization of the *fractal* morphology of fracture surfaces. It is now well established that these surfaces, for very different types of materials such as steels (Mandelbrot et al., 1984; Imre et al., 1992; Måløy et al., 1992), intermetallic alloys (Bouchaud et al., 1993), aluminium alloys (Bouchaud et al., 1990), ceramics (Mecholsky et al., 1989; Måløy et al., 1992), glass (Daguier et al., 1997), various rocks (Schmittbuhl et al., 1993; Plouraboué et al., 1995; Schmittbuhl et al., 1995) and various species of wood (Engoøy et al., 1994; Morel et al., 1998), exhibit self-affine scaling properties in a large range of lengthscales. For instance, by using simultaneously scanning electron microscopy and atomic force microscopy, Daguier et al. (1996) have shown that the self-affine fractal domain, could extend over five decades of lengthscales in the case of a Ti<sub>3</sub>Al-based alloy. More recently, the only use of scanning electron microscopy could lead to the same conclusion on an aluminum alloy (Hinojosa et al., 1999). In most studies, the self-affine fractal domain is characterized by a scaling exponent  $\zeta_{loc}$  (called the local roughness exponent) which drives the evolution of the fluctuations of heights as a function of the lengthscale of observation. Note that the fractal dimension  $d_F$  is simply obtained from the local roughness exponent  $\zeta_{loc}$  through the expression  $d_F = 3 - \zeta_{loc}$ . An outstanding finding is that, in most cases and in spite of strong differences in the materials, a local roughness exponent  $\zeta_{loc} \simeq 0.8$  has been measured. This robustness of the results seems to support the idea suggested by Bouchaud et al. (1990) that the local roughness exponent might be a universal value, i.e., independent of the fracture mode and of the material.

Nevertheless, if the value of the local roughness exponent  $\zeta_{loc}$  seems universal, the range of lengthscales within which the self-affine scaling domain is observed strongly depends on the material microstructure. Moreover, recent studies focussed on the complete description (3D) of the scaling properties of fracture surfaces obtained in two quasi-brittle materials (granite: López and Schmittbuhl, 1998; wood: Morel et al., 1998) have shown the anisotropy of the scaling laws governing the development of the fracture surface in the directions parallel and perpendicular to the direction of crack propagation.

Let us summarize the main results obtained in wood (Morel et al., 1998) from the mode I fracture tests described in the previous section. As previously mentioned, the crack surfaces were generated along the average radial-longitudinal plane of wood. In this particular fracture plane and for a crack propagation in the longitudinal direction, the usual toughening mechanisms of wood such as crack bridging and fiber pull-out are almost non-existent and so,

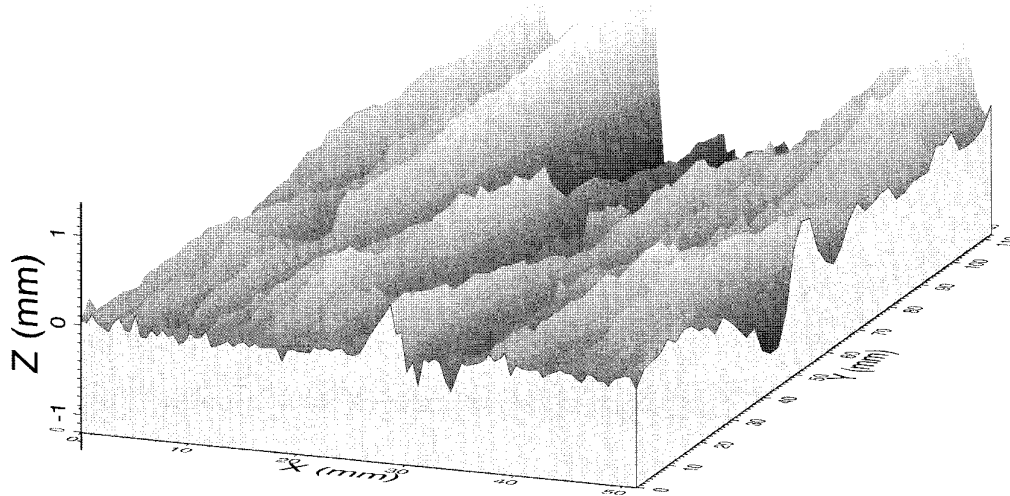


Figure 5. Map of a crack surface (around  $10^4$  data points) obtained on a Pine specimen of width  $L = 60$  mm. The straight notch was initially oriented along the  $x$  axis. As the distance  $y$  to the initial notch increases, the roughness develops up to 3 mm.

confer a relative *cleanness* to the fracture surfaces. Topographies of the fracture surfaces were recorded with a mechanical profiler along regular grids oriented along the  $x$  direction, parallel to the initial notch. The  $y$  direction corresponds to the direction of crack propagation. The step of sampling in the  $x$  direction was adjusted to the cell width ( $\Delta x = 25\mu\text{m}$ ) and to the cell length in the  $y$  direction ( $\Delta y = 2.5$  mm). For each map, the first profile ( $y = 0$ ) is sampled in the immediate vicinity of the initial straight notch and hence corresponds approximately to a zero roughness. One of the maps recorded on a Maritime pine specimen is shown in Figure 5. Morel et al. (1998) have found that the roughness  $\Delta h(l, y)$  of the crack surfaces characterized by the root mean square of the height fluctuations estimated over a window of size  $l$  along the  $x$  axis (i.e., along a profile) and at a distance  $y$  from the initial notch, exhibits particular scaling properties, called *anomalous scaling* in the statistical physics literature (Schroeder et al., 1993; Das Sarma et al., 1994; López and Rodríguez, 1996; López et al., 1997), such as

$$\Delta h(l, y) \simeq A \begin{cases} l^{\zeta_{\text{loc}}} \xi(y)^{\zeta - \zeta_{\text{loc}}} & \text{if } l \ll \xi(y)^\zeta, \\ \xi(y)^\zeta & \text{if } l \gg \xi(y)^\zeta. \end{cases} \quad (3.1)$$

A schematic representation of this anomalous scaling is given in Figure 6. According to (3.1), if one considers one isolated profile parallel to the initial notch (i.e., for  $y = cte$ ),  $\xi(y)$  corresponds to the self-affine correlation length along the  $x$ -axis below which the profile appears to be self-affine. In other terms, the correlation length  $\xi(y)$  can be considered as the *size of the fractal motif*. Thus, for lengthscales  $l \ll \xi(y)$ , the scaling of the height fluctuations is driven by the local roughness exponent  $\zeta_{\text{loc}}$  such as

$$\Delta h(l \ll \xi(y), y = cte) \simeq (A \xi(y)^{\zeta - \zeta_{\text{loc}}}) l^{\zeta_{\text{loc}}}, \quad (3.2)$$

where the term between brackets can be considered as a prefactor of the self-affine scaling relation and  $A$  is a material-dependent constant. For lengthscales  $l \gg \xi(y)$ , the magnitude

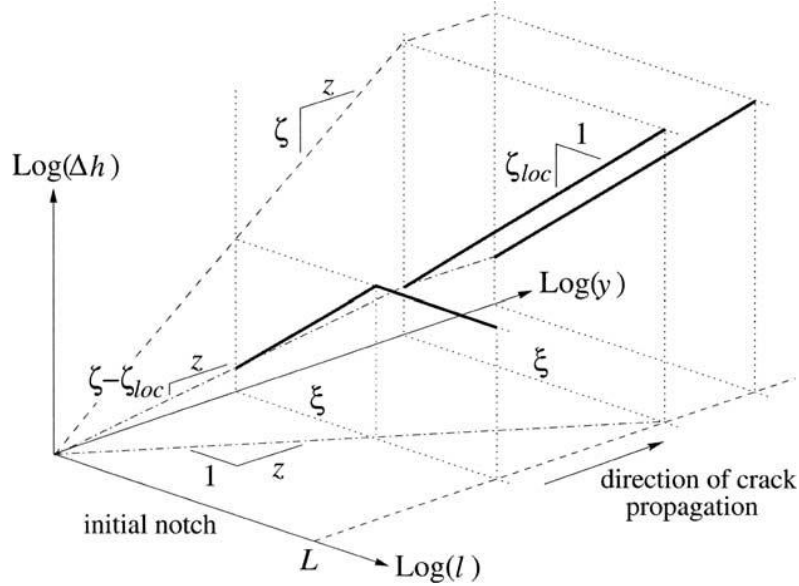


Figure 6. Schematic representation of the anomalous scaling of crack roughness (Equation (3.1)).

of the roughness remains constant and saturates as  $\Delta h(l, y = cte) \simeq A\xi(y)^\zeta$  where the exponent  $\zeta$  is called global roughness exponent (López et al., 1997).

Moreover, the self-affine correlation length  $\xi(y)$  evolves as a function of the distance to the initial notch  $y$  such as  $\xi(y) \simeq By^{1/z}$  where  $z$  is the dynamic exponent and  $B$  is a second material-dependent constant. Thus, if one considers each profile, the magnitude of the roughness measured for a small length scale  $l \ll \xi(y)$  evolves as a power law according to the distance to the initial notch

$$\Delta h(l \ll \xi(y), y) \simeq (AB^{\zeta-\zeta_{loc}} l^{\zeta_{loc}})^{(\zeta-\zeta_{loc})/z}. \quad (3.3)$$

It has been found in wood (Morel et al., 1998) that the magnitude of the roughness increases from the initial notch according to (3.1) until the self-affine correlation length  $\xi(y)$  reaches its maximum value  $\xi_{\max}$  at a certain distance  $y_{\text{sat}}$  from the notch :  $\xi(y \gg y_{\text{sat}}) = \xi_{\max}$ . This implies that the first growth regime of the roughness (i.e., for  $y \ll y_{\text{sat}}$ ) is followed by a stationary regime (for  $y \gg y_{\text{sat}}$ ) where the magnitude of the roughness remains constant. The saturation state of the roughness appears at approximately ten millimeters from the initial notch in the case of the small specimens ( $L = 11.25$  mm) while for the biggest specimens ( $L = 60$  mm) about ten centimeters are required to reach the stationary regime. Moreover, it has been shown that a linear relationship exists between the maximum length  $\xi_{\max}$  and the specimen size  $L$ :  $\xi_{\max} = CL$  where  $C$  is a constant. The maximum size of the fractal motif characterized by the maximum correlation length  $\xi_{\max}$  is found to be about 10 or 20% of the width of the specimens. According to (3.2), the relation  $\xi_{\max} \sim L$  leads to an outstanding specimen size dependence of the roughness magnitude at saturation

$$\Delta h(l, y \gg y_{\text{sat}}) \sim l^{\zeta_{loc}} L^{\zeta-\zeta_{loc}}. \quad (3.4)$$

From the analysis of wood fracture surfaces (Morel et al., 1998), estimates of the local roughness exponents are :  $\zeta_{\text{loc}} = 0.87 \pm 0.07$  for Spruce and  $\zeta_{\text{loc}} = 0.88 \pm 0.07$  for Pine

which are consistent with the conjecture of a universal local roughness exponent (Bouchaud et al., 1990). The global roughness exponents  $\zeta$  have also been measured :  $\zeta = 1.60 \pm 0.10$  for Spruce and,  $\zeta = 1.35 \pm 0.10$  for Pine. The values of the dynamic exponent  $z$  are found to fall between  $2.0 \pm 0.3$  and  $5.9 \pm 0.3$  in the case of Spruce and  $1.8 \pm 0.3$  and  $4.3 \pm 0.3$  in the case of Pine. However, in spite of the scattering of these values,  $z$  seems to be independent of the specimen size. These results can be compared with those obtained on granite (López and Schmittbuhl, 1998) where the exponents  $\zeta_{loc} = 0.79$ ,  $\zeta = 1.2$  and  $z = 1.2$  were obtained. From results obtained in these two experimental studies (López and Schmittbuhl, 1998; Morel et al., 1998), it has been suggested that the global roughness exponent  $\zeta$  and the dynamic exponent  $z$ , which seem to be material-dependent, could be good candidates to characterize the material properties (Morel et al., 1998).

In conclusion, expressions (2.3) and (3.3) emphasize respectively the anisotropy of the crack developments along the directions perpendicular and parallel to the direction of crack propagation. Hence, the fractal dimension  $d_F$  (which is only obtained from the local roughness exponent  $\zeta_{loc}$ ) is not sufficient to characterize the morphology of a fracture surface when exists an anomalous roughening. Nevertheless, the fractal dimension characterizes partly the morphology of an isolated profile, but it does not describe the prefactor (3.2).

#### 4. Fracture criterion in the case of a rough crack

In the following, we consider the problem of fracture for a single rough crack. This is a simplified problem for quasibrittle materials because of the existence of the fracture process zone and especially the mechanisms of energy dissipation which are associated. Nevertheless, although the energy dissipated in microcracking is not taken into account by the present approach, it is interesting to see how the morphology of the main crack alone can be linked to the fracture mechanisms.

As previously mentioned in Section 2, in a quasibrittle material, a LEFM approach is admissible in the sense of the formulation of an equivalent linear elastic problem. This is the frame of the previous connections between the fractal nature of cracks and the fracture properties proposed by Bažant (1997) and Borodich (1997). In the same way, we propose to use the Griffith criterion in order to estimate the energy released by a rough crack, but in introducing a complete description of the fracture surface morphology and especially the roughness development at the onset of fracture. Let us consider a semi-infinite linear elastic specimen of thickness  $L$  containing an initial crack  $a = a_0 + \Delta_a$  and submitted to an uniaxial tension (mode I). In the classical Griffith approach, the fracture criterion is established from the balance of the elastic energy released at the macroscale during an infinitesimal crack propagation and the energy required to create the corresponding free surfaces at the microscale. According to LEFM, the rate of energy dissipation in the structure as a whole is defined with respect to the projected crack surface  $A_p$  since at the macroscale, the roughness of the crack surface can be ignored. On the contrary, the estimate of the energy required for crack propagation at the microscale needs to take into account the real crack surface  $A_r$ . Thus,  $G$  being the elastic energy release rate at the macroscale during an infinitesimal crack advance  $\delta a$ , the fracture criterion can be written as:

$$\underbrace{G\delta A_p}_{\text{macroscale}} = \underbrace{2\gamma\delta A_r}_{\text{microscale}}, \quad (4.1)$$

where  $\delta A_r$  is the real crack surface produced during the infinitesimal crack advance  $\delta a$  and  $\delta A_p = L\delta a$  is the projected crack surface onto the average crack plane. The term  $\gamma$  is the so-called specific surface energy. Note that the specific surface energy is generally considered as a material dependent constant. However, for an heterogeneous material,  $\gamma$  fluctuates spatially. In the above expression,  $\gamma$  has the meaning of an average value.

To estimate the real surface  $\delta A_r$ , we consider the actual surface produced by the advance of a *virtual* crack front as proposed in Morel et al. (2000). This virtual front is defined as a fracture profile (Section 3). This means that only its out-of-plane roughness is considered – the reference plane being the average fracture plane –, and that its projection onto that plane is parallel to the initial notch. The real crack surface  $\delta A_r$  produced during the infinitesimal crack extension  $\delta a$  can be estimated as follows:

$$\delta A_r \simeq \int_{\Delta a}^{\Delta a + \delta a} \psi(y) dy, \quad (4.2)$$

where  $\psi(y)$  is the extended length of the virtual crack front at a distance  $y$  from the initial notch. A first-order approximation, which consists in considering that during the small crack extension  $\delta a$  the length of the mean crack front  $\psi$  does not evolve (i.e.,  $\psi(\Delta a + \delta a) = \psi(\Delta a) + \Omega(\delta a)$  where  $\lim \Omega(\delta a) = 0$  for  $\delta a \rightarrow 0$ ), leads to the following expansion of the fracture criterion (Morel et al., 2000)

$$G = 2\gamma \frac{\psi(y)}{L}. \quad (4.3)$$

From (4.3), the energy release rate  $G$  is proportional to the ratio  $\psi(y)/L$  which can be considered as a roughness factor of the virtual crack front.

We estimate the extended length  $\psi$  of the mean crack front from the morphological description of the fracture surface given by the anomalous scaling (3.1). This description includes the development of the crack roughness which is significantly different from the previous approaches (Bažant, 1997, Borodich, 1997).

#### 4.1. ANOMALOUS ROUGHENING AND CONSEQUENCES ON THE CRACK FRONT LENGTH

According to (3.1), the function  $\Delta h(l, y)$  considered for a particular position  $y$ , can be seen as a description of a virtual crack front along the  $x$  axis located at the distance  $y$  from the initial notch. Moreover, this virtual front is a self-affine curve the projection of which along the  $x$  axis corresponds to the specimen width  $L$ .

The real length  $\psi$  of the virtual front is estimated by covering the front path with segments of length  $\delta$  (Figure 7). The horizontal ( $x$  axis) and vertical ( $z$  axis) projections of the segments are according to (3.1) equal to  $l_0$  and to  $A\xi(y)^{\xi - \xi_{loc}} l_0^{\xi_{loc}}$ , respectively. The length  $l_0$  corresponds to the lower cutoff of the fractal range, i.e., to the characteristic size of the smaller micro-structural element. In mechanical terms, this lower cutoff corresponds to the smallest microstructural element involved in the fracture process. The length of the segment  $\delta$  can be expressed as:

$$\delta \simeq l_0 \sqrt{1 + \left( \frac{A\xi(y)^{\xi - \xi_{loc}}}{l_0^{1 - \xi_{loc}}} \right)^2}. \quad (4.4)$$

In Equation (4.4), the ratio between brackets corresponds to the tangent of the angle between the segment  $\delta$  and the  $x$  axis. A self-affine fracture surface does not exhibit overhangs

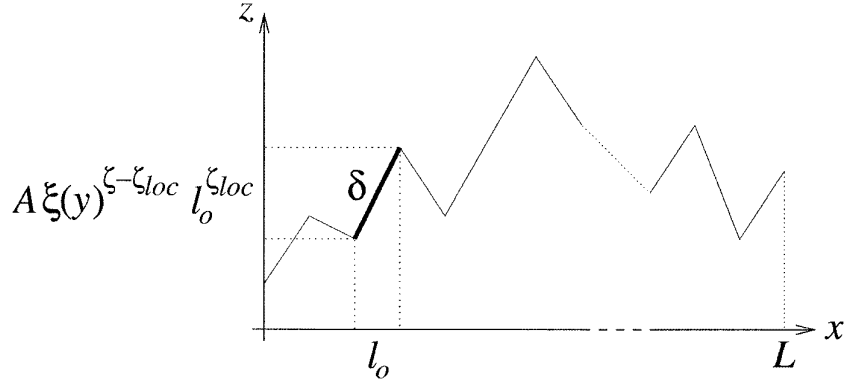


Figure 7. Measurement of the length of the crack front with segments  $\delta$  of horizontal projected length  $l_0$  (lower cutoff) and vertical projected length  $A \xi(y)^{\zeta - \zeta_{loc}} l_0^{\zeta_{loc}}$ . The number of segments  $\delta$  needed to cover the curve is estimated by the ratio  $(L/l_0)$ . The length  $\psi$  of the crack front is :  $\psi = (L/l_0)\delta$ .

and so the number of segments  $\delta$  needed to cover the mean crack front curve is equal to  $L/l_0$ . As a consequence, as shown in Morel et al. (2000), the actual length  $\psi$  of the virtual front depends on the distance  $y$  to the initial notch

$$\psi(y) \simeq L \begin{cases} \left[ 1 + \left( \frac{A(B y^{1/z})^{\zeta - \zeta_{loc}}}{l_0^{1 - \zeta_{loc}}} \right)^2 \right]^{1/2} & \text{if } y \ll y_{sat}, \\ \left[ 1 + \left( \frac{A(C L)^{\zeta - \zeta_{loc}}}{l_0^{1 - \zeta_{loc}}} \right)^2 \right]^{1/2} & \text{if } y \gg y_{sat}. \end{cases} \quad (4.5)$$

From the initial notch, the length of the virtual crack front  $\psi(y)$  first increases as a power law of the distance  $y$  to the initial notch. It remains constant and proportional to the specimen width  $L$  in the zone where the roughness saturates (i.e., for  $y \gg y_{sat}$ ). Note that the length of the self-affine fractal curve (4.5) is a finite quantity in contrast to the expressions proposed by Carpinteri (1994), Borodich (1997) and Bažant (1997) where there is no lower cutoff for the fractal curves and accordingly infinite lengths.

#### 4.2. R-CURVE BEHAVIOR

Consider now a crack of length  $a = a_0 + \Delta a$  where  $a_0$  is the length of the initial notch and  $\Delta a = y$  corresponds to the crack length increment. In the zone where the roughness grows (i.e., where  $\Delta a \ll \Delta a_{sat}$ , with  $\Delta a_{sat} = y_{sat}$ ), it has been shown by Morel et al. (2000) that the fracture equilibrium (4.3) leads to an energy release rate function of the crack length increment  $\Delta a$

$$G_R(\Delta a \ll \Delta a_{sat}) \simeq 2\gamma \sqrt{1 + \left( \frac{AB^{\zeta - \zeta_{loc}}}{l_0^{1 - \zeta_{loc}}} \right)^2} \Delta a^{2(\zeta - \zeta_{loc})/z}. \quad (4.6)$$

In Equation (4.6), the subscript  $R$  in  $G_R$  emphasizes that the behavior of the resistance to fracture is similar to an R-curve behavior (Lawn, 1993). This evolution is driven by the progressive increase of the roughness factor  $\psi/L$ . In other terms, the fracture equilibrium

(4.3) leads to an equivalent surface tension (related to the projected crack surface) depending on the crack length increment  $\Delta a$  :  $\gamma'(\Delta a) = \gamma\psi(\Delta a)/L$ . In this expression, the roughness factor  $\psi(\Delta a)/L \geq 1$  can be seen as a toughening term. The resistance  $G_R$  starts from  $2\gamma$  (at the onset of the fracture) and the increase of the toughening term as a function of the crack length increment  $\Delta a$  induces an apparent growth of the resistance  $G_R$ . On the other hand, when the crack increment is large, i.e., for  $\Delta a \gg \Delta a_{\text{sat}}$  which corresponds to the saturation state of the roughness, the resistance to fracture can be expressed in the following way

$$G_{RC}(\Delta a \gg \Delta a_{\text{sat}}) \simeq 2\gamma \sqrt{1 + \left(\frac{A}{l_0^{1-\zeta_{\text{loc}}}}\right)^2} (CL)^{2(\zeta - \zeta_{\text{loc}})}. \quad (4.7)$$

The subscript  $C$  in  $G_{RC}$  (4.7) indicates that the energy release rate, obtained in the zone where the roughness magnitude saturates, corresponds to an asymptotic or *critical* resistance to crack growth. Indeed, when the roughness saturates, the roughness factor  $\psi/L$  has reached its maximum value and induces a resistance to crack growth which is independent of the crack length increment  $\Delta a$  (Morel et al., 2000). In this stationary regime, the toughening mechanisms have reached their maximum intensity, leading to a post  $R$ -curve propagation at constant resistance for  $\Delta a \gg \Delta a_{\text{sat}}$ . The post  $R$ -curve regime at constant resistance to crack growth (4.7) corresponds to the one which is generally assumed in the phenomenological approaches of the  $R$ -curve behavior (Bažant, 1984; Bažant and Kazemi, 1990; and See Lawn, 1993, for a more detailed review of the phenomenological approaches). The fracture energy obtained in (4.6) and (4.7) are in agreement with the classical dimensions of LEFM contrary to those obtained in Carpinteri (1994), Borodich (1997) and Ba zant (1997) where an unconventional definition of fracture energy, called *fractal fracture energy*, is required.

In Figures 8 and 9 are plotted some examples of the experimental resistances to crack growth obtained respectively on Norway Spruce and Maritime Pine specimens and fitted with the  $R$ -curve (4.6) and post  $R$ -curve (4.7) behaviors. Note that the fit is obtained in keeping three free parameters : the specific surface energy  $\gamma$ , the ratio  $A/l_0^{1-\zeta_{\text{loc}}}$  and the scaling exponent  $(\zeta - \zeta_{\text{loc}})/z$ . The expected  $R$ -curve behavior (4.6) provides a good description of the increase of the experimental resistances to crack growth. When the roughness analysis have been performed (Morel et al., 1998), the measured exponents  $(\zeta - \zeta_{\text{loc}})/z$  given between brackets in Figures 8 and 9 are close to those obtained from the fit. For the other specimens, the fitted values of  $(\zeta - \zeta_{\text{loc}})/z$  are consistent with the measured values from the roughness analysis (Section 3). Note that the fits of the phenomenological resistance curves need the use of an overestimated ratio  $A/l_0^{1-\zeta_{\text{loc}}}$  if compared to the one obtained from the experimental estimates of  $A$  and  $l_0$ . The experimental value of the material constant  $A$  can be estimated from Equation (4.5) by computing the experimental lengths of topographic profiles while the value of  $l_0$ , fixed by the step of sampling of the topographic profiles ( $l_0 = \Delta x = 25 \mu\text{m}$ ), corresponds to the cell width of wood (Section 3). Nevertheless, the real value of  $l_0$  (related theoretically to the lower cutoff of the fractal range) might be smaller than the cell width. Indeed, during the fracture process, some cell walls break revealing a microstructure at smaller lengthscales. However, experimental estimates of topographies at small lengthscales are impossible with the profiler technology used in Morel et al. (1998). Moreover, the values of the specific surface energy  $2\gamma$  if compared to the critical energy release rates  $G_{RC}$  indicate a strong toughening mechanism ( $G_{RC} \gg 2\gamma$ ) in wood. This toughening appears more pronounced in Martime Pine than in Norway Spruce.

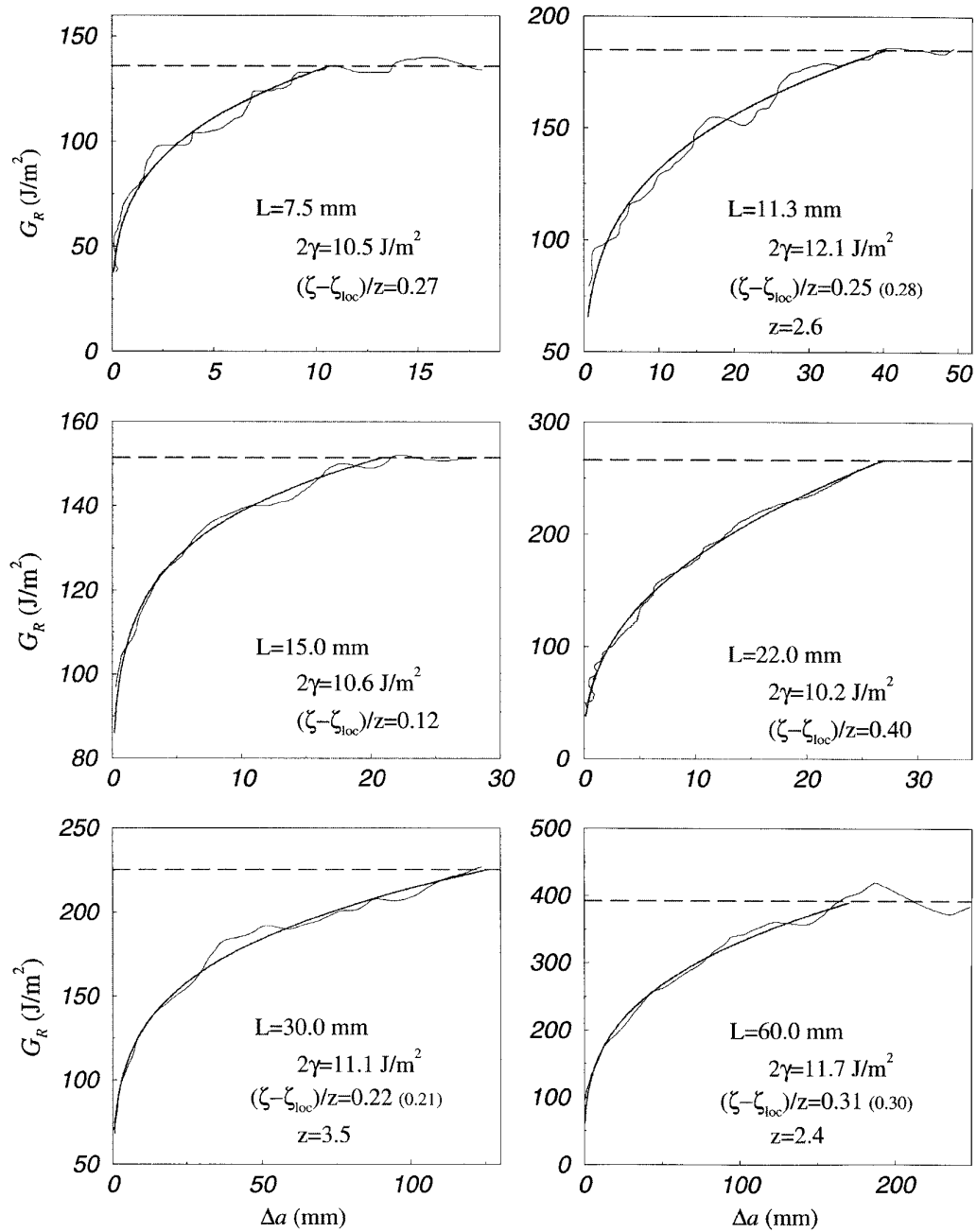


Figure 8. Some fits of the phenomenological R-curves obtained in the case of Norway Spruce obtained from (4.6) and (4.7). The specific surface energy  $2\gamma$  and the exponent  $(\zeta - \zeta_{loc})/z$  are obtained from the fit. The values of  $(\zeta - \zeta_{loc})/z$  given in brackets are the expected values from the roughness analysis.

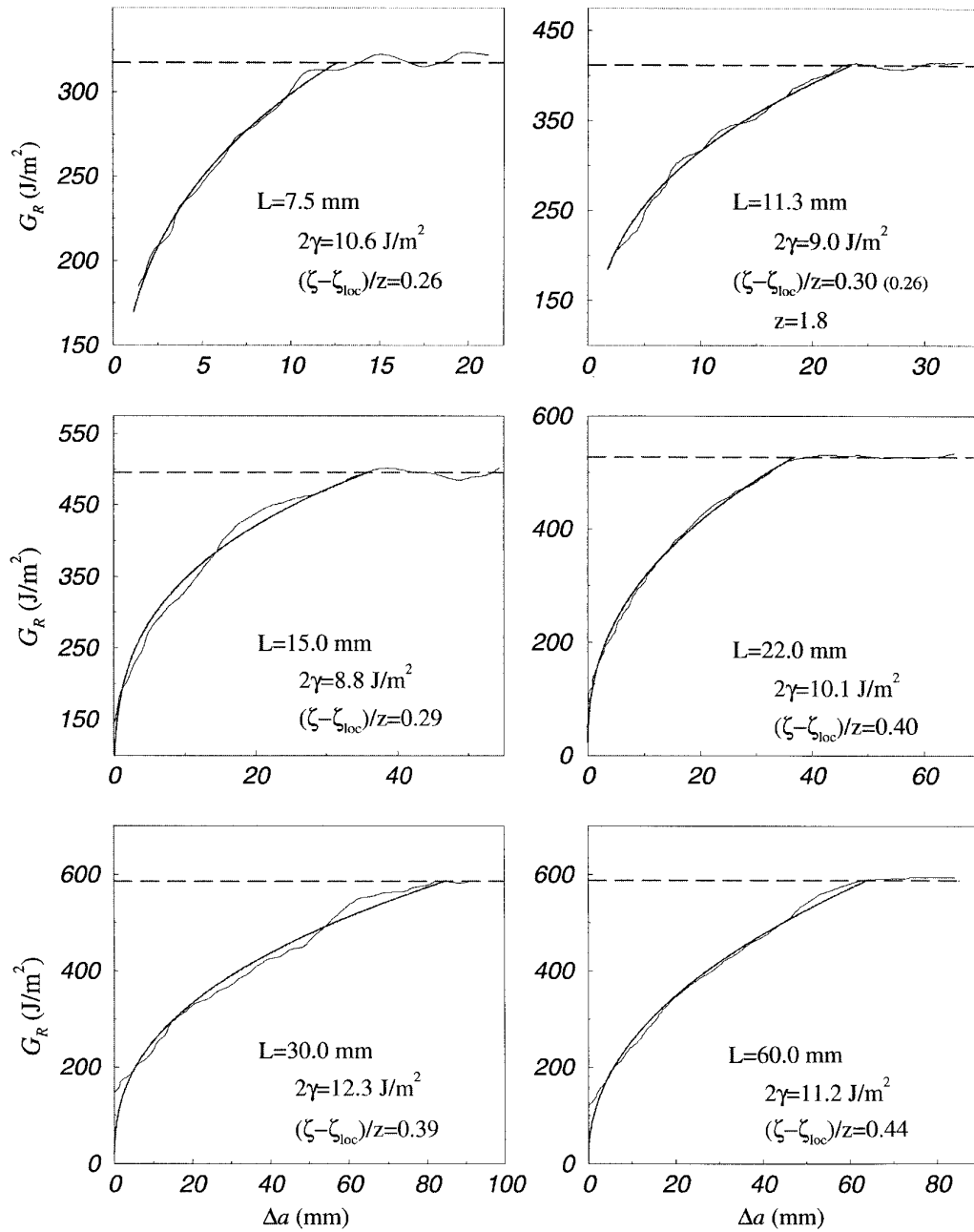


Figure 9. Fits of the phenomenological  $R$ -curves obtained in the case of Maritime Pine obtained from (4.6) and (4.7).

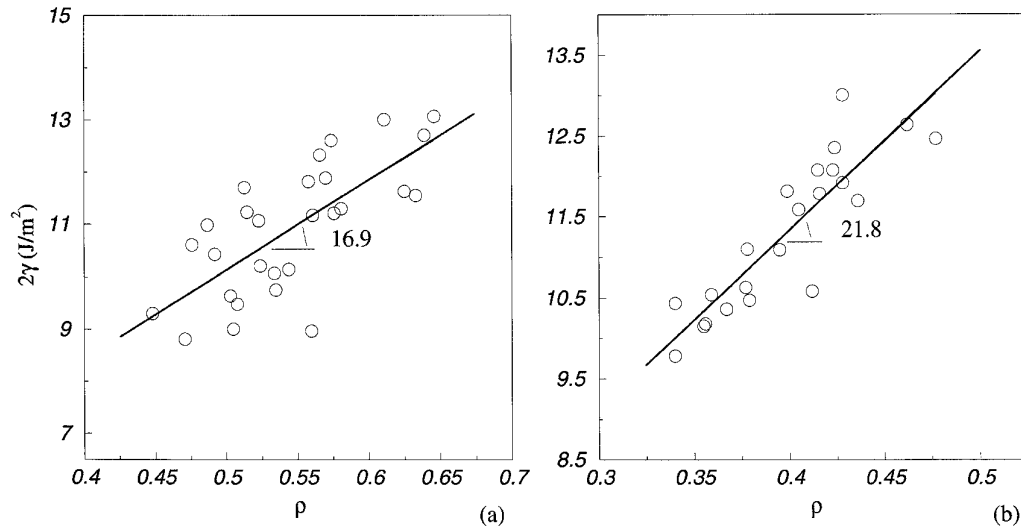


Figure 10. Specific surface energy  $2\gamma$  (obtained from  $R$ -curve fits) versus the oven dry specific density  $\rho$  measured on Maritime Pine (a) and Norway Spruce (b).

For both wood species, the specific surface energy seems to depend on the oven dry specific density  $\rho$  measured on each specimen. Figures 10a and 10b show the values of the specific surface energy  $2\gamma$  as a function of  $\rho$ , for Maritime Pine and Norway Spruce, respectively. Figure 10 illustrates the variability of the mechanical characteristics with respect to a characteristic microstructural parameter.

#### 4.3. SIZE EFFECT

As previously mentioned in Section 1, size effect is the main characteristic of the fracture behavior of quasibrittle materials such as concrete, rocks or wood (see Bažant and Kazemi, 1990, and references therein). The link between the morphology of crack surfaces and the material fracture properties, established in the previous section, leads to a size effect on the critical resistance  $G_{RC}$  as shown in (4.7).

In Figure 11, the theoretical evolution of the critical resistance (4.7) is plotted as a function of the characteristic size  $L$  for the arbitrary values :  $\zeta = 1.3$ ,  $\zeta_{loc} = 0.8$ ,  $A = 0.1$ ,  $C = 1$  and  $l_0 = 1$ . It appears that the size effect on  $G_{RC}/2\gamma$  shows a transition between two asymptotic behaviors, respectively,  $G_{RC} = 2\gamma$  and  $G_{RC} \sim L^{\zeta - \zeta_{loc}}$ . The transition between the asymptotic behaviors takes place at a crossover length  $L_c = 1/C(l_0^{1 - \zeta_{loc}}/A)^{1/(\zeta - \zeta_{loc})}$ . For small specimen sizes, i.e.,  $L \ll L_c$ , there is no size effect :  $G_{RC} \simeq 2\gamma$ . For these small specimens, the crack surfaces are expected to be ‘shallow’, i.e., the average local angle of the crack profile is smaller than 45 deg. Hence, the real crack surfaces being weakly different from the projected one, the classical conditions of LEFM are satisfied and the energy release rate related to the projected surfaces are close to the specific surface energy  $2\gamma$ . For large specimen sizes  $L \gg L_c$ , the critical resistance evolves as a power law :  $G_{RC} \sim L^{\zeta - \zeta_{loc}}$ . The fracture surfaces of these large specimen are ‘spiky’ (i.e., the average local angle of the crack profile overpasses 45 deg) and lead to critical energy release rates larger than the specific surface energy. This size effect is due to the fact that the average local angle determined in the zone where the roughness saturates is function of the specimen size. Indeed, from Equation (3.4), if one considers the

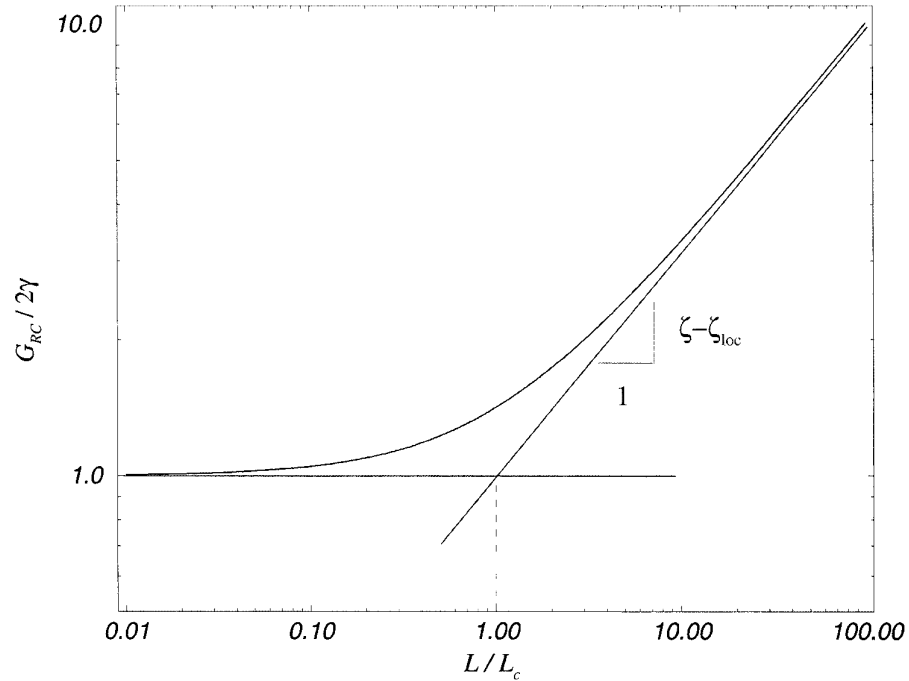


Figure 11. Theoretical size effect on the critical resistance to crack growth (4.7) :  $G_{RC}/2\gamma = \sqrt{1 + (L/L_c)^{2(\zeta - \zeta_{loc})}}$  where the crossover length  $L_c = 1/C(l_0^{1-\zeta_{loc}}/A)^{1/(\zeta - \zeta_{loc})}$ .

tangent of the local angle as the ratio of the typical height fluctuation (i.e., expressed for  $l = l_0$ ) over the lengthscale  $l_0$ , this tangent scales as  $\Delta h(l_0, y \gg y_{sat})/l_0 \sim L^{\zeta - \zeta_{loc}}$ .

The power-law behavior  $G_{RC} \sim L^{\zeta - \zeta_{loc}}$  is in good agreement with the observed size effect in wood as shown in Figure 3. Indeed, the power law fits of the experimental energy release rates (Section 2) are characterized by the exponents  $\alpha$  equal to 0.42 for Pine compared to the expected result  $\zeta - \zeta_{loc} = 1.35 - 0.88 = 0.47 \pm 0.17$ , and  $\alpha = 0.73$  for Spruce for the expected exponent  $\zeta - \zeta_{loc} = 1.60 - 0.87 = 0.73 \pm 0.17$ . In fact, the local angles measured on the wood fracture surfaces are smaller than 45 deg but the crossover lengths  $L_c$  estimated from the ratio  $A/l_0^{1-\zeta_{loc}}$  obtained from the  $R$ -curve fits (Figures 8 and 9) for both wood species are smaller than the sizes  $L$  of tested specimens. This justifies the use of the power law  $G_{RC} \sim L^{\zeta - \zeta_{loc}}$ . Experimental estimates of strong local slopes at small lengthscales are difficult to observe anyway because of the technology used for the recording of the topographic profiles. As a matter of fact, in Morel et al. (1998), profiles are recorded with a spherical needle moving along the fracture surfaces. The shape and the volume of the needle induce a geometric filter at small lengthscales, and sharp hills or holes are not correctly recorded. However, despite of the limited range of sizes used, the relation (4.7) is in very good agreement with the experimental observations.

Moreover, the curve plotted in Figure 11 can be seen as the evolution of the maximum toughening effect as a function of the specimen size  $L$ . For large specimens (i.e.,  $L \gg L_c$ ), the toughening mechanisms are important and so, the critical energy release rates measured at the macroscopic level are larger than the specific surface energy (i.e.,  $G_{RC}/2\gamma \gg 1$ ). For

small specimens, the toughening being insignificant, the exact conditions of LEFM are almost verified and hence, the resistance to crack growth is close to the specific surface energy  $2\gamma$ .

The scaling effect in wood, and more particularly the effect of structure size on its nominal strength, could be explained by such a difference between the energy release rates of small and large structures.

## **5. Conclusion**

We have investigated the idea that the toughening in quasibrittle materials could be linked to the roughness of fracture surfaces. Despite the fact that the development of the fracture process zone implies energy dissipation, we have considered the propagation of a single crack in order to estimate the contribution of the main crack roughness to the toughening mechanism.

From the results of two previous experimental studies describing the complete scaling behavior of the fracture surfaces of quasibrittle materials (granite in López and Schmittbuhl, 1998, and wood in Morel et al., 1998), we have shown that the fractal dimension alone is not sufficient to characterize the morphology of the crack surfaces and especially at the onset of fracture. On the basis of an anomalous scaling, we have investigated the idea proposed by Bažant (1997) and Borodich (1997) which consists in estimating the elastic energy released at the macroscale by a rough crack at the microscale.

The growth of the roughness at the onset of crack propagation leads to an *R*-curve behavior which is followed by a propagation at a constant fracture resistance in the zone where the roughness saturates. It appears that, from the results obtained for the fracture of wood specimens, measured and predicted resistance curves collapse nicely. Moreover, we have shown that the main consequence of this link between the morphology of crack surfaces and the material fracture properties is a size effect on the *R*-curves. This size effect results from the link between the roughness magnitude of fracture surfaces and the specimen size and leads to a size effect on the critical resistance to crack growth. The expected size effect is consistent with the experimental results obtained on the critical energy release rates for wood.

The fracture behavior estimated on the basis of an anomalous scaling accounts for an *R*-curve behavior and a size effect on the critical resistance. Hence, the anomalous roughening of fracture surfaces seems to reflect the behavior of brittle heterogeneous materials exhibiting toughening mechanisms. If the energetical contribution of the actual free surfaces cannot explain alone the complete fracture behavior, the scaling exponents characterizing the roughening provide nevertheless an estimate of the evolution of the toughening effect in quasibrittle materials. The knowledge of the toughening evolution (as a function of the equivalent crack length) and of the size effect on the maximum toughening intensity provide good descriptions of the *R*-curve behavior and of the scaling of the critical resistance to crack growth. Ongoing experimental studies attempt to link systematically fracture behaviors and crack roughening for various quasibrittle materials.

## **Acknowledgements**

We are particularly grateful to J.R. Rice for fruitful discussions and enlightening remarks. This work was partly supported by the CNRS-ECODEV project.

## References

- Balankin, A.S. (1996). The effect of fracture surface morphology on the crack mechanics in a brittle material. *International Journal of Fracture* **76**, R63–R70
- Bažant, Z.P. (1984). Size effect in blunt fracture : concrete, rock, metal. *J. Eng. Mech. ASCE* **110**, 518–535.
- Bažant Z.P. and Kazemi, M.T. (1990). Size effect in fracture of ceramics and its use to determine fracture energy and effective process zone length. *J. Am. Ceram. Soc.* **73**, 1841–1853, and references therein.
- Bažant, Z.P. (1997). Scaling of quasibrittle fracture: hypotheses of invasive and lacunar fractality, their critique and Weibull connection. *International Journal of Fracture* **83**, 41–65, and references therein.
- Borodich, F.M. (1997). Some fractal models of fracture. *Journal Mechanics Physics and Solids* **45**, 239–259, and references therein.
- Bouchaud, E. (1997). Scaling properties of cracks. *J. Phys. Cond. Mat.* **9**, 4319.
- Bouchaud, E. and Bouchaud, J.-P. (1994). Fracture surfaces : apparent roughness, relevant length scales, and fracture toughness. *Phys. Rev.* **B50**, 17752–17755.
- Bouchaud, E., Lapasset, G. and Planés, J. (1990). Fractal dimension of fractured surfaces : a universal value? *Europhys. Lett.* **13**, 73–79.
- Bouchaud, E., Lapasset, G., Planés, J. and Navéos, S. (1993). Statistics of branched fracture surfaces. *Phys. Rev.* **B48**, 2917–2928.
- Brenich, A. and Carpinteri, A. (1998). Stress field interaction and strain energy distribution between a stationary main crack and its process zone. *Eng. Fract. Mech.* **59**, 797–814.
- Carpinteri, A. (1994). Scaling laws and renormalization groups for strength and toughness scaling of disordered materials. *Int. J. Solids Struct.* **31**, 291–302.
- Daguier, P., Hénaux, S., Bouchaud, E. and Creuzet, F. (1996). Quantitative analysis of a fracture surface by atomic force microscopy. *Phys. Rev. E* **53**, 5637–5642.
- Daguier, P., Nghiem, B., Bouchaud, E. and Creuzet, F. (1997). Pinning/Depinning of crack fronts in heterogeneous materials. *Phys. Rev. Lett.* **78**, 1062–1065.
- Das Sarma, S., Ghaisas, S.V. and Kim, J.M. (1994). Kinetic super-roughening and anomalous dynamic scaling in nonequilibrium growth models. *Phys. Rev.* **E49**, 122–125.
- Dauskardt, R.H., Haubensak, F. and Ritchie, R.O. (1990). On the interpretation of the fractal character of fracture surfaces. *Acta Metall. Mater.* **38**, 143–159.
- Ducourthial, E., Bouchaud, E. and Chaboche, J.-L. (2000). Influence of microcracks on the propagation of macrocracks. *Computational Mat. Sci.* **19**, 229–234.
- Engøy, T., Måløy, K.J., Hansen, A. and Roux, S. (1994). Roughness of two- dimensionnal cracks in wood. *Phys. Rev. Lett.* **73**, 834–837.
- Feder, J. (1988). *Fractals*. Plenum Press, New-York.
- Hinojosa, M. and Bouchaud, E. (1999). Unpublished.
- Hori, M. and Nemat-Nasser, S. (1987). Interacting micro-cracks near the tip in the process zone of a macro-crack. *J. Mech. Phys. Solids* **35**, 601–629.
- Imre, A., Pajkossy, T. and Nyikos, L. (1992). Electrochemical determination of the fractal dimension of fractured surfaces. *Acta Metall. Mater.* **40**, 1819–1826.
- Kachanov, M. (1994). Elastic solids with many cracks and related problems. *Advances in Applied Mechanics* **30**, 259–445.
- Lawn, B.R. (1993). *Fracture of Brittle Solids*, 2nd ed. Cambridge University Press, Cambridge.
- López, J.M. and Rodríguez, M.A. (1996). Lack of self-affinity and anomalous roughening in growth processes. *Phys. Rev.* **E54**, R2189–R2192.
- López, J.M. and Schmittbuhl, J. (1998). Anomalous scaling of fracture surfaces. *Phys. Rev.* **E57**, 6405–6409.
- López, J.M. and Rodríguez, M.A., Cuerno, R. (1997). Superroughening versus intrinsic anomalous scaling of surfaces. *Phys. Rev.* **E56**, 3993–3998.
- Måløy, K.J., Hansen, A., Hinrichsen, E.L. and Roux, S. (1992). Experimental measurements of the roughness of brittle cracks. *Phys. Rev. Lett.* **68**, 213–215.
- Mandelbrot, B.B., Passoja, D.E. and Paullay, A.J. (1984). Fractal character of fracture surfaces of metals. *Nature* **308**, 721–722.
- Mecholsky, J.J., Passoja, D.E. and Feinberg-Ringel, K.S. (1989). Quantitative analysis of brittle fracture surfaces using fractal geometry. *J. Am. Ceram. Soc.* **72**, 60–65.

- Morel, S., Schmittbuhl, J., López, J.M. and Valentin, G. (1998). Anomalous roughening of wood fractured surfaces. *Phys. Rev.* **E58**, 6999–7005.
- Morel, S. (1998). *Effet d'échelle dans la rupture d'un matériau hétérogène (le bois)*. Thèse de doctorat de l'université Bordeaux I.
- Morel, S., Schmittbuhl, J., Bouchaud, E. and Valentin, G. (2000). Scaling of crack surfaces and implications for fracture mechanics. *Phys. Rev. Lett.* **85**, 1678–1681.
- Mosolov, A.B. (1993). Mechanics of fractal cracks in brittle solids. *Europhys. Lett.* **24**, 673–678.
- Plouraboué, F., Kurowski, P., Hulin, J.P., Roux, S. and Schmittbuhl, J. (1995). Aperture of rough cracks. *Phys. Rev.* **E51**, 1675.
- Schmittbuhl, J., Gentier, S. and Roux, S. (1993). Field measurements of the roughness of fault surfaces. *Geophysics Res. Lett.* **20**, 639–641.
- Schmittbuhl, J., Schmitt, F. and Scholz, C. (1995). Scaling invariance of crack surfaces. *Geo. Res.* **100**, 5953–5973.
- Schroeder, M., Siegert, M., Wolf, D.E., Shore, J.D. and Plischke, M. (1993). Scaling of growing surfaces with large local slopes. *Europhys. Lett.* **24**, 563–568.